ADVANCED MATERIALS

[7] a) P. Bäuerle, T. Fischer, B. Bidlingmeier, A. Stabel, J. P. Rabe, *Angew. Chem. Int. Ed. Engl.* **1995**, *34*, 303. b) A. Stabel, J. P. Rabe, *Synth. Met.* **1994**, *67*, 47.
[8] a) H. Müller, J. Petersen, R. Strohmaier, B. Gompf, W. Eisenmenger, M. S. Vollmer, F. Effenberger, *Adv. Mater.* **1996**, *8*, 733. b) M. S. Vollmer, F. Effenberger, R. Stecher, B. Gompf, W. Eisenmenger, *Chem. Eur. J.* **1999**, *5*, 96.
[9] A. MacEachern, C. Soucy, L. C. Leitch, J. T. Arnason, P. Morand, *Tetrahedron* **1988**, *44*, 2403.
[10] C. Böhm, Forschungspraktikum, Universität Stuttgart **1996**.
[11] P. Bäuerle, F. Würthner, G. Götz, F. Effenberger, *Synthesis* **1993**, 1099.

Dependence of Elastic Properties on Morphology in Single-Wall Carbon Nanotubes**

By *Oleg Lourie*, *H. Daniel Wagner*,* *Yaogang Zhang*, and *Sumio Iijima*

Single-wall carbon nanotubes (SWNTs) may well be used in a variety of future applications[1–5] due to their versatile and promising electronic and mechanical properties. Most stimulating is the fact that the material properties of small-diameter nanotubes are predicted to exhibit quantum size effects, based on their symmetry (chirality) and diameter. For example, their electronic and magnetic properties are predicted to be diameter-dependent,[4] and their conductivity may vary from metallic to semiconducting, depending on their chiral symmetry.[6–9] This was experimentally confirmed by recent scanning tunneling microscopy (STM) studies.[10,11] A fascinating issue is whether a similar interdependence between the mechanical properties and the microstructure (diameter, chirality) of SWNTs is possible.[12–14] For a given chirality, the stiffness of SWNTs is predicted to decrease with decreasing diameter,[12] and for a given diameter, the stiffness should increase with increasing chiral angle.[12] For nanotubes that are packed into ropes or that have larger diameters, these dependences are expected to be more complex, and a sharp decrease in stiffness is predicted for SWNTs with diameters above 1.5 nm.[14] Additional theoretical research[15–17] and recent transmission electron microscopy (TEM)[18–20] and atomic force microscopy (AFM)[21,22] work also support the apparent exceptional mechanical properties of carbon nanotubes in general, but without experimental evidence, so far, of a relationship between their morphology (diameter and chirality) and the mechanical properties.

[*] Prof. H. D. Wagner, Dr. O. Lourie
Department of Materials and Interfaces
Weizmann Institute of Science
Rehovot 76100 (Israel)
Dr. Y. Zhang, Prof. S. Iijima
Fundamental Research Laboratories, NEC Corporation
34 Miyukigaoka, Tsukuba, Ibaraki 305-8501 (Japan)

[**] This project was supported in part by a grant from the Minerva Foundation, and in part by the Israel Science Foundation founded by the Israel Academy of Sciences and Humanities. The authors are grateful to Prof. O. Navon (The Hebrew University of Jerusalem) for the use of a Renishaw Ramascope with a 514.5 nm laser line.

In the present study we induced a compressive deformation in SWNTs embedded into a polymer matrix by cooling a specimen to 81 K. We showed in earlier work[23] that such deformation may be monitored by the Raman D*-band frequency shift of the embedded nanotubes. Here we find that such compressive shift strongly depends on the laser excitation wavelength. Because it was recently found that the Raman excitation frequency can be chosen to preferentially excite nanotubes of a particular diameter, we interpret our observations in terms of a possible correlation between elastic properties and geometry of carbon nanotubes, as is now described.

The specimens used in the present study were made of an epoxy resin (Araldite LY564, Ciba-Geigy, hardener HY560) and SWNT ropes prepared by a laser ablation method.[24–26] The preparation of the composite specimens is fully described elsewhere.[23] Raman spectra were obtained with a Renishaw Ramascope equipped with a Linkam THMS 600 cooling cell. The spectra were collected with a spectral resolution of 1 cm^{-1} in the backscattering mode, using the 780 nm line of a AlGaAs diode laser, the 632.8 nm line of a helium–neon laser, and the 514.5 nm line of an argon laser. The nominal powers of these lasers were 20, 25, and 12 mW, respectively. A Lorentzian-fitting function was used to obtain band position and intensity.[23] Compressive stresses were induced in the nanotubes from the shrinkage of the polymer matrix due to polymerization, and by further quenching of the specimen to a temperature of 81 K.[23] The latter was performed by injecting nitrogen gas from a liquid nitrogen reservoir through the thermally isolated cooling cell fitted to the Raman microscope stage.

Raman spectra of SWNTs in air (thus, not embedded) were first generated, using three different excitation wavelengths (Fig. 1). Three prominent sets of peaks are observed in the low- (≈200 cm^{-1}), middle- (≈1600 cm^{-1}), and high-frequency (≈2600 cm^{-1}) regions. The low-frequency band represents the combination of A_{1g} and E_{1g} vibrational modes. The main feature in the middle-frequency region,

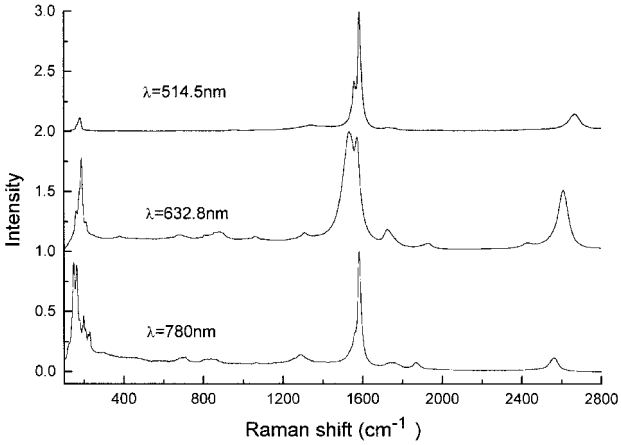

Fig. 1. Raman spectra of SWNTs in air at T = 295 K using three excitation wavelengths. The changes in intensity, shape, and position of the spectra features are due to diameter-selective Raman scattering [27] (see text).

  0935-9648/99/1108-0931 $ 17.50+.50/0

the G band, is composed of A_{1g}, E_{1g}, and E_{2g} vibrational modes, and the most intense band in the high-frequency region is the D^* band, which is an overtone of the disorder-induced D band (≈1300 cm^{-1}), having an A_{1g}-type vibrational symmetry.[27,28,29] As seen in Figure 1, varying the excitation wavelength induces dramatic changes in the intensity of the low-frequency band. The intensity increases with increasing laser wavelength, in rough agreement with earlier observations by Rao et al.[27] The intensity variations in the mid-frequency region are less notable, although peak broadening and shape alteration are observed for the G band, especially in the spectrum generated with the helium–neon laser. In the high-frequency part of the spectrum (which was not studied by Rao et al.[27]), we observe a significant shift toward lower wavelengths in the position of the D^* band (Fig. 1, full line in Fig. 2, and Table 1) as the laser excitation wavelength increases. A similar large

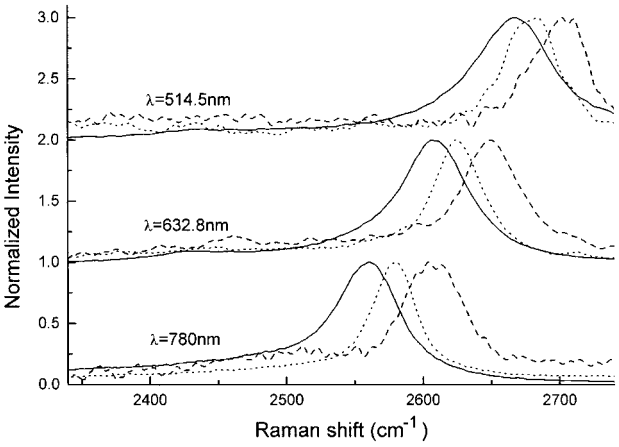

Fig. 2. Effect of embedment and cooling on the frequency shift of the D^* band of SWNTs using three excitation wavelengths: solid line, SWNTs in air at T = 295 K; dotted line, embedded SWNTs at T = 295 K; dashed line, embedded SWNTs at T = 81 K (band intensities were normalized to emphasize frequency shifts).

Table 1. Observed compressive shift of the D^* band of SWNTs. $\langle\omega\rangle$ denotes the average frequency of the D^* band at temperature T [K] and excitation wavelength λ [nm].

Specimen	Excitation wavelength λ [nm]	Temperature T [K]	Observed frequency of D^* band $\langle\omega\rangle \pm \sigma$ [cm^{-1}] [a]	Total shift Δ [cm^{-1}]
SWNT in air	780	296	2560.2 ± 1.4	
SWNT in air	780	81	2566.8 ± 2.2	
				Δ = -48.4
Embedded SWNT	780	296	2578.8 ± 1.7	
Embedded SWNT	780	81	2608.6 ± 1.5	
SWNT in air	632.8	296	2609.0 ± 2.0	
SWNT in air	632.8	81	2613.0 ± 2.0	
				Δ = 41.3
Embedded SWNT	632.8	296	2626.9 ± 0.6	
Embedded SWNT	632.8	81	2650.3 ± 0.6	
SWNT in air	514.5	296	2667.8 ± 0.7	
SWNT in air	514.5	81	2672.0 ± 0.5	
				Δ = 31.3
Embedded SWNT	514.5	296	2677.5 ± 3.4	
Embedded SWNT	514.5	81	2699.1 ± 2.5	

[a] σ = standard deviation.

shift was seen by Rao et al.[27] in the lower-frequency range, on variation of the laser frequency, for small-diameter nanotubes. They interpreted such a positional shift as evidence for diameter-selective coupling of the SWNTs to the exciting radiation field. Briefly, the electronic structure of a SWNT is dictated by its geometry.[6–9] For small-diameter armchair SWNTs, the gap between the singularities in the electronic density of states (DOS) is inversely proportional to the diameter (Fig. 4 in the paper by Rao et al.[27]). Raman scattering becomes resonant, if the energy of the incident photons corresponds to one of the gaps in the DOS. A SWNT specimen is usually composed of nanotubes with different geometries,[10,11,30] and the resonance condition for a certain type of SWNT will be defined by how closely the excitation laser energy, and the nanotube electronic structure, match. Thus, from the Raman data, it is possible in principle to determine the most probable diameter in a given population.

Following the embedment of the nanotubes in the polymer matrix, we observe that the D^* band exhibits a shift toward higher frequencies (dotted line in Fig. 2) at all three excitation wavelengths. The upshift is a consequence of embedment in the polymer,[23] which results in nanotube compression. A further upshift is observed for the three lasers when quenching to 81 K (Table 1). We observe that the magnitude of the total shift (due to both embedment in the matrix and subsequent quenching) is found to increase with increasing excitation wavelength (Table 1). A similar but smaller effect is also found for the G band.

Based on the correlation between the band shift and bond length shortening,[23] it is possible to calculate the compressive strain of the nanotubes as shown in Equation 1, where ω_0 and ω_q are bond frequencies before and after quenching. Equation 1 is an approximation in general, but it is accurate in single-shell nanotubes for which bond shortening and the overall tube deformation are directly proportional. As shown in Figure 3, the compressive strain—and thus the compliance—of SWNTs increases as a function of the excitation frequency. This mechanical property may be correlated with the diameter of the nanotubes, as is now discussed.

$$\varepsilon_{nt} = -\left(1 - \frac{\omega_0}{\omega_q}\right) \quad (1)$$

The literature concerning the morphological aspects of nanotubes produced by laser ablation may briefly be summarized as follows. TEM and Raman studies predict that in such nanotubes, the armchair type seems to be dominant,[27] which is also consistent with electron diffraction and nanotube coalescence studies.[25,31–33] However, recent STM studies[10,11] show that various degrees of chirality may, nevertheless, arise in SWNTs produced by the same method,[24–26] and that a rather narrow distribution of diameters (between 1.1 and 1.5 nm, corresponding to (8,8) to (11,11) tube symmetries) is predicted.[27,25,31,32] The DOS is apparently only weakly affected by chirality, and mainly

  0935-9648/99/1108-0932 $ 17.50+.50/0

ADVANCED MATERIALS

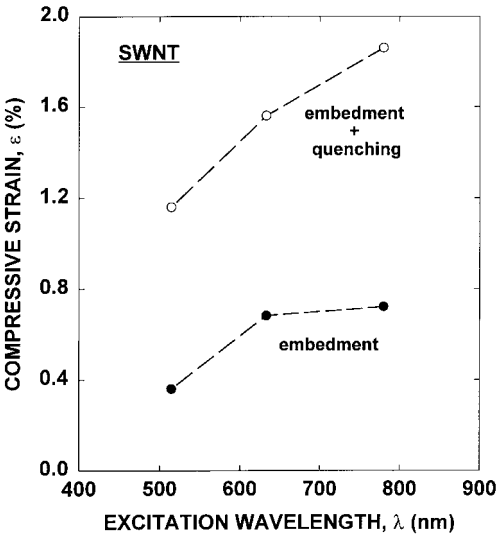

Fig. 3. Compressive strain of SWNTs (calculated from observed frequency shifts of the D* band) against excitation wavelength, resulting from embedment in a polymer matrix (closed circles) and from combined embedment and temperature quenching (open circles).

depends on the diameter of the SWNT.[34,35] Thus, the role of chirality distribution on the resonant Raman effect observed in SWNTs may be only secondary. Due to the "merging" of singularities in the DOS[36] of larger diameter, any resonant Raman effect will be relatively difficult to observe for chiral nanotubes. As a side remark, it is worth noting that, unlike the radial "breathing" modes[37,38] (corresponding to the low-frequency part of the Raman spectrum in Fig. 1), which were suppressed on nanotube embedment in the polymer, the axial "breathing" modes (corresponding to the D* band) are unaffected by embedment.

In view of the above, and the fact that the Raman spectra of the SWNTs studied here (Fig. 1) closely match the patterns predicted for (*n*,*n*) nanotubes,[27] we may assume that the SWNTs indeed possess armchair symmetry. The laser excitation wavelength of 780 nm (1.58 eV) exactly corresponds to the first-order transition of an (8,8) nanotube as calculated with a tight binding model (see Fig. 4 in Rao et al.[27]). The 514.5 nm (2.41 eV) laser excitation wavelength fits well (but not exactly) with the second-order transition of a (10,10) nanotube (equal to 2.38 eV). The laser line, 632.8 nm, (1.95 eV) might correspond to either a first-order transition with an *n* value lower than 8, or to a second-order transition with an *n* value higher than 11, or to a value averaged over the nanotube population. The diameters of (7,7) and (12,12) nanotubes are 0.95 and 1.6 nm, respectively (using the relationship $d = 1.357n$, where d is the diameter in Angstroms), i.e., rather displaced from the mean of the SWNT diameter distribution. Because the diameter distribution in the specimen is narrow,[27,25,31,32] such nanotube types should be present only in very small quantities. This, however, is not consistent with our Raman observations, which show broad spectra features for that laser line (Fig. 1). Hence, if the armchair symmetry is dominant as assumed, the observed Raman spectrum excited with the wavelength of 632.8 nm is probably the average response arising from a range of tube diameters.

In view of the selectivity of the excitation frequency toward specific nanotube types, as just discussed, and the increasing compressive strain of SWNTs as a function of the excitation frequency, we conclude that the compliance of the (8,8) SWNT is significantly larger than that of the (10,10) nanotubes. In other words, SWNTs of the (*n*,*n*) type become softer with decreasing diameters. This experimental observation is in general agreement with theoretical predictions.[12,14,39] More specifically, although Lu[40] predicts that the elastic moduli of carbon nanotubes should be insensitive to structural details, others[12,39] predict a strong dependence on diameter at small diameters, reaching a constant limiting behavior at about 1.2 nm. Similarly, Tersoff and Ruoff[14] predict a strong increase in the modulus up to 1.5 nm, but tubes with greater diameters exhibit tube distortion characteristics. The relevant tube diameter range in the present work is 1.09 to 1.36 nm, for which the relatively strong experimental variation observed in Figure 3 seems to confirm Tersoff and Ruoff's prediction. The compressive strain calculated for the 632.8 nm laser line is intermediate between the results for the two other laser lines (Fig. 3) and is thus consistent with this conclusion.

In summary, we have shown that diameter-selective resonance Raman scattering can be employed to sense the elastic properties of armchair SWNTs having different diameters. A strict interpretation of this effect is necessarily related to both the diameter and chirality of nanotubes, although theoretical predictions suggest that for armchair tubes chirality may have no effect on the elastic properties. The observed dependence of the SWNT compressibility on the excitation wavelength can be regarded as experimental evidence of a correlation between the elastic properties of SWNTs and their diameter. It is worth pointing out that the experimental correlation presented here is only indirect; direct evidence will be produced only when tube populations with well-controlled geometries become available.

Received: January 5, 1999
Final version: April 20, 1999

[1] S. Iijima, T. Ichihashi, *Nature* **1993**, *363*, 603.
[2] D. S. Bethune, C. H. Kiang, M. S. de Vries, G. Gorman, R. Savoy, J. Vazquez, R. Beyers, *Nature* **1993**, *363*, 605.
[3] T. W. Ebbesen, *Carbon Nanotubes*, CRC Press, Boca Raton, New York **1997**.
[4] M. S. Dresselhaus, G. Dresselhaus, P. C. Eklund, *Science of Fullerenes and Carbon Nanotubes*, Academic, New York **1996**.
[5] B. I. Yakobson, R. E. Smalley, *Am. Sci* **1997**, *85*, 324.
[6] J. W. Mintmire, B. I. Dunlap, C. T. White, *Phys. Rev. Lett.* **1992**, *68*, 631.
[7] N. Hamada, S. Sawata, A. Oshiyama, *Phys. Rev. Lett.* **1992**, *68*, 1579.
[8] R. A. Jishi, M. S. Dresselhaus, G. Dresselhaus, *Phys. Rev. B* **1993**, *48*, 11 385.
[9] R. Saito, M. Fujita, G. Dresselhaus, M. S. Dresselhaus, *Appl. Phys. Lett.* **1992**, *60*, 2204.
[10] J. W. G. Wildoer, L. C. Venema, A. G. Rinzler, R. E. Smalley, C. Dekker, *Nature* **1998**, *391*, 59.
[11] T. W. Odom, J.-L. Huang, P. Kim, C. M. Lieber, *Nature* **1998**, *391*, 62.

  0935-9648/99/1108-0933 $ 17.50+.50/0

[12] D. H. Robertson, D. W. Brenner, J. W. Minmire, *Phys. Rev. B* **1992**, *45*, 12 592.
[13] S. Sawada, N. Hamada, *Solid State Commun.* **1992**, *83*, 917.
[14] J. Tersoff, R. S. Ruoff, *Phys. Rev. Lett.* **1994**, *73(5)*, 676.
[15] G. Overney, W. Zhong, D. Z. Tomanek, *Z. Phys. D* **1993**, *27*, 93.
[16] B. I. Yakobson, C. J. Brabec, J. Bernholc, *Phys. Rev. Lett.* **1996**, *76*, 2511.
[17] S. Iijima, C. Brabec, A. Maiti, J. Bernholc, *J. Chem. Phys.* **1996**, *104*, 2089.
[18] M. M. J. Treacy, T. W. Ebbesen, J. M. Gibson, *Nature* **1996**, *381*, 678.
[19] H. D. Wagner, O. Lourie, Y. Feldman, R. Tenne, *Appl. Phys. Lett.* **1998**, *72*, 188.
[20] O. Lourie, D. M. Cox, H. D. Wagner, *Phys. Rev. Lett.* **1998**, *81*, 1638.
[21] E. W. Wong, P. E. Sheehan, C. M. Lieber, *Science* **1997**, *277*, 1971.
[22] M. R. Falvo, G. J. Clary, R. M. Taylor II, V. Chi, F. P. Brooks, Jr., S. Washburn, R. Superfine, *Nature* **1997**, *389*, 582.
[23] O. Lourie, H. D. Wagner, *J. Mater. Res.* **1998**, *13*, 1.
[24] T. Guo, P. Nikolaev, A. Thess, D. T. Colbert, R. E. Smalley, *Chem. Phys. Lett.* **1995**, *243*, 49.
[25] A. Thess, R. Lee, P. Nikolaev, H. Dai, P. Petit, J. Robert, C. Xu, Y. H. Lee, S. G. Kim, D. T. Colbert, G. Scuseria, D. Tomanek, J. R. Fisher, R. E. Smalley, *Science* **1996**, *273*, 483.
[26] Y. Zhang, H. Gu, K. Suenaga, S. Iijima, *Chem. Phys. Lett.* **1997**, *279*, 264.
[27] A. M. Rao, E. Richter, S. Bandow, B. Chase, P. C. Eklund, K. A. Williams, S. Fang, K. R. Subbaswamy, M. Menon, A. Thess, R. E. Smalley, G. Dresselhaus, M. S. Dresselhaus, *Science* **1997**, *275*, 187.
[28] F. Tuinstra, J. L. Koenig, *J. Chem. Phys.* **1970**, *53*, 1126.
[29] J. M. Holden, P. Zhou, X.-X. Bi, P. C. Eklund, S. Bandow, R. A. Jishi, K. D. Chowdhury, M. S. Dresselhaus, G. Dresselhaus, *Chem. Phys. Lett.* **1994**, *220*, 186.
[30] M. S. Dresselhaus, *Nature* **1998**, *391*, 19.
[31] J. M. Cowley, P. Nikolaev, A. Thess, R. E. Smalley, *Chem. Phys. Lett.* **1997**, *265*, 379.
[32] L.-C. Qin, S. Iijima, H. Kataura, Y. Maniwa, S. Suzuki, Y. Achiba, *Chem. Phys. Lett.* **1997**, *268*, 101.
[33] P. Nikolaev, A. Thess, A. G. Rinzler, D. T. Colbert, R. E. Smalley, *Chem. Phys. Lett.* **1997**, *266*, 422.
[34] C. T. White, J. W. Mintmire, *Nature* **1998**, *394*, 29.
[35] J.-C. Charlier, P. Lambin, *Phys. Rev. B* **1998**, *57*, R15037.
[36] R. Saito, T. Takeya, T. Kimura, G. Dresselhaus, M. S. Dresselhaus, *Phys. Rev. B* **1998**, *57*, 4145.
[37] R. Saito, T. Takeya, T. Kimura, G. Dresselhaus, M. S. Dresselhaus, *Phys. Rev. B* **1999**, *59*, 2388.
[38] M. A. Pimenta, A. Marucci, S. A. Empedocles, M. G. Bawendi, E. B. Hanlon, A. M. Rao, P. C. Eklund, R. E. Smalley, G. Dresselhaus, M. S. Dresselhaus, *Phys. Rev. B* **1998**, *58*, R16016.
[39] E. Hernandez, C. Goze, P. Bernier, A. Rubio, *Phys. Rev. Lett.* **1998**, *80*, 4502.
[40] J. P. Lu, *Phys. Rev. Lett* **1997**, *79*, 1297.

Microtribology and Direct Force Measurement of WS_2 Nested Fullerene-Like Nanostructures**

By *Yuval Golan*,* *Carlos Drummond*, *Moshe Homyonfer*, *Yishai Feldman*, *Reshef Tenne*, and *Jacob Israelachvili*

While experiments did not confirm earlier speculations on exceptional lubrication behavior of carbon-based fullerenes, inorganic fullerene-like nested nanostructures (IFs) were recently reported to show improved tribological behavior when added to lubricant fluids.[1] In this report, we confirm the tribological advantages of WS_2 IFs as additives to tetradecane between two shearing mica surfaces, and show that the lower friction in this system is associated with friction-induced material transfer of WS_2 from the IFs to the mica surfaces. While the material transfer occurs via delamination and structural degradation of the IFs, their addition to conventional lubricant fluids provides an effective route for in situ deposition of an ultrathin solid lubricant coating on the shearing surfaces.

Spherical molecules such as C_{60} and C_{70} were speculated to have tribological advantages due to their high frequency rotation in the solid lattice, which would allow them to act as molecular ball bearings at shearing interfaces. Nevertheless, despite the large number of experimental studies, this issue remains controversial. Addition of C_{60} to fluid lubricants has been shown to dramatically reduce the viscous drag at the solid–liquid interface,[2–5] and other earlier studies reported encouraging results.[6,7] On the other hand, organic fullerene-based solid lubricant films were reported to show disappointing friction and wear properties,[8–10] failed to produce coatings of commercial value,[11] and fullerene additives were reported to offer no advantage over conventional additives.[12]

Coatings of Mo and W chalcogenides were reported to be effective solid lubricants[13] which exhibit a prolonged wear life.[14] The tribological properties were shown to be highly sensitive to the atmosphere due to chemical reactions with oxygen and water under shearing conditions.[15–18] While the low friction of metal chalcogenide solid lubricants is often explained by the facile shear of the *c*-planes of the 2H lattice, this mechanism cannot explain their unusually long

[*] Dr. Y. Golan,[+] C. Drummond, Dr. J. Israelachvili
Department of Chemical Engineering, and Materials Department
University of California
Santa Barbara, CA 93106 (USA)
M. Homyonfer, Y. Feldman, Dr. R. Tenne
Department of Materials and Interfaces
The Weizmann Institute of Science
Rehovot 76100 (Israel)

[+] From fall 1999: Department of Materials Engineering, Ben Gurion University, Beer Sheva 84105 (Israel)

[**] This work made use of the MRL Central Facilities supported by the NSF under award DMR-9123048. J.I. acknowledges the support of the Office of Naval Research for supporting this research under Grant N00014-93-1-0269. R.T. acknowledges the support of the ACS-PRF foundation (USA) and the US–Israel Binational Science Foundation.

  0935-9648/99/1108-0934 $ 17.50+.50/0